

Retinopathy of Prematurity Detection in Infants using Gamma Transformation and Gabor Wavelet on Tiles of Retinal Images

*SeyedAliakbar Mousavi^{#1}, Zahra Hanifeloo^{#2}, Putra Sumari^{#3}, Muhammad RafieMohd Arshad^{#4}

[#] School of Computer Science, Universiti Sains Malaysia (USM), Malaysia.

*¹ pouyaye@gmail.com

² hanifeloo@live.com

³ putras@cs.usm.my

⁴ rafie@cs.usm.my

Abstract—Retinopathy of prematurity (ROP) is a disease that leads to blindness if the diagnosis is not made on time. Designing an automatic and intelligent system for early diagnosis can prevent the blindness in infants. However, the blood vessels in the retina of infants is less clear, hence the correct diagnosis of vessels is very difficult. In this study, first the pre-processing stage removes the noise of images, after that the images are divided into 16×16 windows and Gabor filter is applied to each sub-window. Energy and entropy are calculated for each sub-window, and finally these features are sent into a neural network to determine whether the sub-window has a vessel or not. By counting the number of sub-windows containing vessel, the prematureness and completeness of retina is determined. In this method, the mean accuracy of images that have been classified is 80.88% respectively.

Retinal vessel extraction, Retinopathy of premature infants, Gabor filters.

I. INTRODUCTION

In recent decades, the images of retina have been widely used in medical associations to identify and investigate the diseases [1,2]. Retinal blood vessels are important structures in retinal images because of the important information and useful parameters that are extracted from them to diagnose the disease and evaluate the eyes. For example, the retinal vessels show some appearance changes of length, diameter, branching of arteries and also vascular disease [3]. Blood vessels are also used as an indicator for evaluation and classification of the disease in each patient's retinal images.

Some pathological lesions such as exudates and micro-aneurysms can be diagnosed by separating the structures of retinal vessels. ROP is an eye disease in premature infants. In infants who are born preterm (premature infants), the growth of vessels is stopped before they can fully cover the retina. The parts that have not vessels, cannot get enough oxygen and food, therefore, it causes the disease. This disease is more common in infants with less than 1500 g weighing and gestational age less than 31 weeks; and if the diagnosis isn't made on time, in short time, it leads to blindness. The purpose of this study is providing a method to determine immaturity or completeness of the infant's eye's retina [4]. The next section presents some of the past studies. In section 3 to 5, the proposed method is presented. In section 6, a discussion about results is presented. Finally, the conclusion is made in section 7.

II. RELATED WORKS

In recent years, many methods have been proposed to extract retinal vessels, for example according to S. Chaudhuri et al. (1989), the vessel model in the image is assumed as a Gaussian curve and by using the filters corresponding to Gaussian model, the "contrast of the background vessel" is improved, then by applying a thresholding, the vessels are zoned. Since the vessels can be at different extensions, the image with 12 kernels, each of them having 15 degrees of rotation, is convolved [5]. Then, for each pixel, the maximum response of 12 filtering is held. The matching filter response will be under local thresholding operation and then the vessels will be revealed. Figure 1 shows the results of applying this algorithm before thresholding.

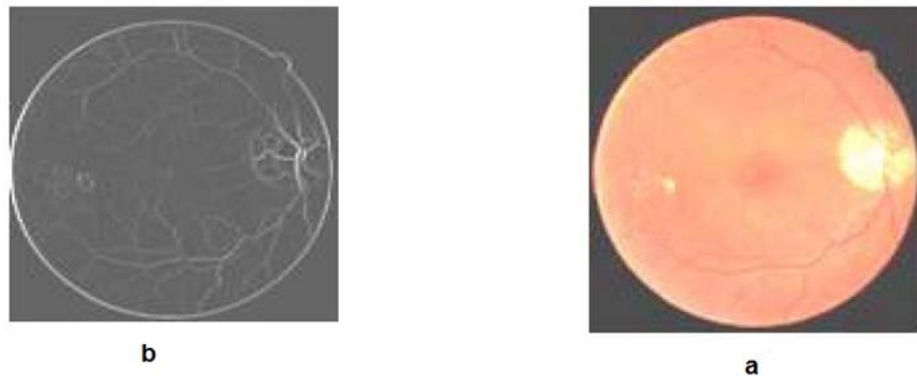


Fig. 1: Algorithm results of Chaudhuri. a: Screenshots b: Extraction of vessels

PBM method (Primitive Based Method) [6] performs the vessels zoning by extracting the ridges from the image which is a good approximation of vessels. These ridges are used for producing the primary features to form the line elements, then the algorithm zones the line into pieces by using the closest element to the image pixels.

A. Fathi et al. (2013) offered an enhancement vessel multi-scale method based on Complex Continuous Wavelet Transform [7]. CCWT parameters are optimized to show the linear structures in all directions and separation of them from the simple edges. The vessels final network is obtained by using a thresholding adaptive histogram-based process with length filtering method. Also, an operator with a circular structure is used to estimate the diameter of the vessels. Performance of these methods on DRIVE and STARE public databases are evaluated and 95% of accuracy, 79% of sensitivity and 97% of specificity was obtained.

A. Fathi et al. (2013) provided a method for detecting the branching points and also measurement of parameters such as vessel diameter, vessel direction and branching angle by using the operator of local model [8]. This method is applied to the DRIVE and STARE public databases and has higher accuracy than the previous algorithms in detecting the blood vessels characteristics.

According to A. Fathi et al. (2013), a multi-scale invariant operator with local binary pattern rotation is used that extracts a feature vector for different types of blood vessels from retinal images [9]. For assessing the vessels in each pixel, the multi-scale feature vector is given to adaptive neuro-fuzzy inference system. After converting the Top-hat, thresholding and length filtering, the thin and thick veins are identified. The efficiency of this approach is measured on the DRIVE and STARE public databases.

J. V. B. Soares et al. (2005) identifies the vessel through changing the angle of rotation and scale parameters in the two-dimensional wavelet transform by using the Morlet wavelet. Morlet wavelet is chosen because it is directed [10]. It means that it is sensitive to the angle conversion and it would identify the vessels that are scattered at different angles.

According to A. Fathi et al. (2014), there is a developed Local Binary Pattern (LBP) method to derive all uniform and non-uniform models by using immutable labeling with spin [11]. Since LBP operator can extract all micro-tissue structures, a new method for automatic improving, monitoring and diagnosis of the blood vessels is obtained through combining it with artificial neural networks. Thinness and thickness of the blood vessels are identified by applying the Top-hat transform and length filtering to the improved blood vessels.

Fraz, M.M., et al. (2011) uses the radial mapping method to locate the central lines of vessels, including the thin vessels [12]. The main idea of this approach is that the mapped curvature of the pixel typically has a peak, if the pixel belongs to the vessel. Then the gradient is used to extract the vascular main structure and the final segmentation is achieved from their aggregation. This method has been implemented on the STARE dataset and the results show that this algorithm is able to identify small vessels in low contrast while the computational cost is very reduced.

A method is provided to estimate and correct the brightness of retinal images. This method uses HSV color space for better combination of brightness and chromatic information. Then, it uses a brightness model on the retina field that solves many of the disadvantages of the previous approaches, especially when there is a big damage in retina. In figure 2, an improved image with this method and the method of averaging is presented and demonstrates that this method provides a better result.

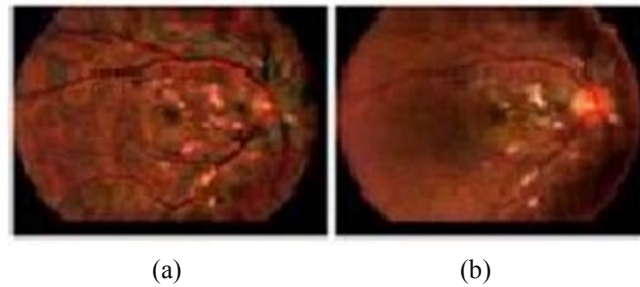


Fig. 2: Correction of the brightness with the averaging method b. Image corrected with method (2)

According to Y. A. Tolias et al. (1998), the c-means fuzzy clustering algorithm is used to follow the vessels in retinal angiogram images [13]. In this method, the area of retina is divided into the "vessel" and "non-vessel" parts. In this method, the pre-processed data are given to the clustering algorithm. This approach also includes some methods to evaluate the validity of diagnosed coronary arteries. According to R. M. Rangayyan et al. (2008), Gabor filters bank is used with adjustable scales which uses 40 pictures to evaluate the performance of the algorithm [14]. The results of the vessel detection technique in the green channel are compared with the images that are drawn manually.

However, the retinal picture of newborns and adults are different in several parameters such as blood vessels clarity, image noise, and veins thickness. These factors make the detection of the infants blood vessels in images difficult. The approaches that have been proposed, have a good response on adults retina images, but these methods usually fail in the retinal images of newborns, especially premature infants. Therefore, these methods, despite the multiplicity and diversity, are not useable to detect the retina vessels in infants.

III. PREPROCESSING

Since the thin vessels brightness is very close to the brightness of the surrounding background, the preprocessing is a very important step in the separation of the vessels. Hence, first we try to find out a threshold for separating the blood vessels from the non-vessels in the image. For this purpose, at first the contrast between the thin vessels and non-vessels is increased by converting gamma which is applied to the green channel reverse of retina's color image [15]. If we show the green channel of the retinal image with fG , the gamma correction for pixel (i, j) is done as follows:

$$fC_{ij} = [(fG_{ij} - fG_{MIN}) / (fG_{MAX} - fG_{MIN})]^2 \quad (1)$$

Where fG_{MIN} and fG_{MAX} are the minimum and maximum values of image brightness and r and fG are the correction parameters. The corrected image is demonstrated by fC .

Since the contrast between the thin vessels and the background is low, the segregation of these arteries, even after applying Gabor filter, is very difficult. To increase the contrast in this areas, the method proposed by J. L. Starck et al. is useable. This method is a linear transformation that is applied to the wavelet coefficients [16]. Equation 2 shows the relationship between wavelet coefficients before and after its filtering.

$$y_c(x) = \begin{cases} 1, & x < c\sigma \\ \frac{x - c\sigma}{c\sigma} \left(\frac{m}{c\sigma}\right)^p + \frac{2c\sigma - x}{c\sigma}, & c\sigma \leq x < 2c\sigma \\ \left(\frac{m}{x}\right)^p, & 2c\sigma x \leq x < m \\ \left(\frac{m}{x}\right)^x, & x \geq m \end{cases} \quad (2)$$

In equation 2, x is the brightness of each pixel in I_c image and $y_c(x)$ is the brightness of same pixel after applying this conversion, and in this transformation, p is a parameter that determines the amount of non-linearity and takes a number between zero and one. ζ defines the range of dynamic compression. If ζ has a non-zero value, while strengthening the weak edges, weakens the stronger edges. c is the normalizing constant and σ is the deviation of the background noise. In equation 2, m is a value that the lights less than this value are boosted; and this value, depending on the brightness values of images pixels, is different for each image. Using the equation 3, the appropriate value for m can be determined by a percentage of maximum brightness in the image and the deviation of the background noise:

$$m = k_c M - c\sigma \quad (3)$$

Figure 3 shows the color image of retina with inverted green channel and the image that artificially grows with the gamma correction is applied to.

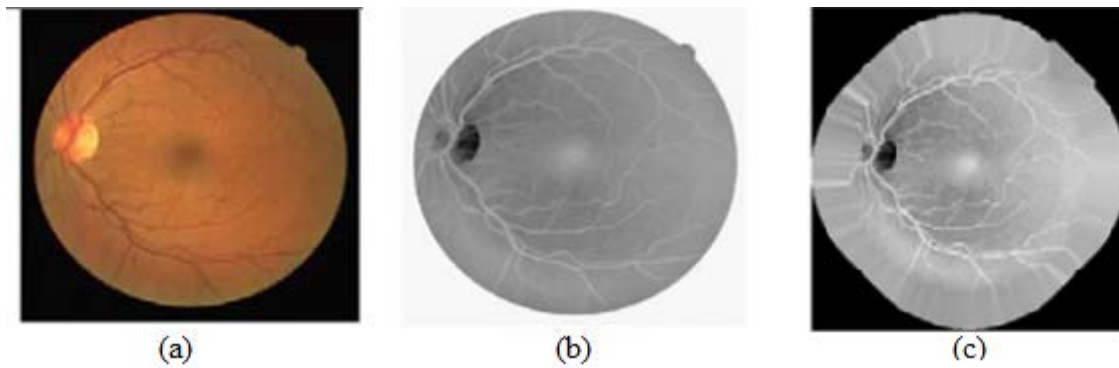


Fig. 3: (a) color image of the retina (b) inverted green channel (c) gamma correction

IV. FEATURE EXTRACTION

After pre-processing, $[16 \times 16]$ windows are removed from the image and Gabor filter is applied to each sub-window. Gabor filters process the image signal in both the spatial and frequency domain and have appropriate texture for related matters. Gabor filters usually used to detect the shapes and extract the features. In the spatial domain, the two-dimensional Gabor filter is composed of a Gaussian core which is modulated by a sine wave, in other words, a Gabor filter is a modulation result of a sine signal with specified frequency and angle in the Gaussian signal and is defined according to equation 6. A filter bank usually consists of Gabor filters with different scales and directions. These filters are Convolve with image and make a Gabor space. Equations 4, 5 show the components of equation 6.

$$h(x, y) = s(x, y) \cdot g(x, y) \quad (4)$$

$$s(x, y) = \exp(-j2\pi(u_0x + v_0y)) \quad (5)$$

In equation 4, $s(x, y)$ is a complex sinusoid and so-called carrier and $g(x, y)$ as shown in equation 4, is the two-dimensional Gaussian function and is called envelope.

$$g(x, y) = \frac{1}{\sqrt{2\pi}\sigma} \exp\left(-\frac{1}{2}\left(\frac{x^2}{\sigma_x^2} + \frac{y^2}{\sigma_y^2}\right)\right) \quad (6)$$

Therefore

$$h(x, y) = e^{-\frac{1}{2}\left(\frac{x^2}{\sigma_x^2} + \frac{y^2}{\sigma_y^2}\right)} \cdot e^{-j2\pi(u_0x + v_0y)} \quad (7)$$

Equation 8 shows Gabor filter frequency response:

$$H(u, v) = \frac{1}{2\pi\sigma_u\sigma_v} \exp\left[-\frac{1}{2}\left[\frac{(u-u_0)^2}{\sigma_u^2} + \frac{(v-v_0)^2}{\sigma_v^2}\right]\right] \quad (8)$$

It is like that we write Gaussian function in a frequency domain in (u_0, v_0) . Therefore, the Gabor filter is a Gaussian function which is shifted to (u_0, v_0) in the frequency domain, in other words, in the distance $\sqrt{u_0^2 + v_0^2}$ from the origin and in the $\tan^{-1} \frac{u_0}{v_0}$ angle. In equation 8, the origin of spatial frequency of the

Gabor filter is (u_0, v_0) . σ_x and σ_y parameters are the standard deviation of the Gaussian function in the x and y directions and determine the bandwidth of the filter. When the picture has lines with the same frequency but in different directions, it is observed that the filter at a specific θ angle, has stronger response. We can obtain all

elements of the picture that their energy is focused on (u_0, v_0) by passing the image from the $(u_0, v_0, \sigma_x, \sigma_y)$ Gabor filter parameters [17,18].

According to the above equation and the definition of Gabor filters, choosing its parameters is one of the major problems in using these filters. In other words, the accuracy of the performed analyses through the Gabor filter depends on its angle, that is determined by the focal point and its variances. There are two approaches for choosing the parameters of Gabor filter. In the first method, called the supervised method, the parameters are determined in advance and the filters are applied to the image signal with predetermined parameters. However, in the second method or the unsupervised method, the parameters are not determined at first and the optimal parameters are achieved by testing a set of them, although it imposes more computational and memory load on the system [19]. There have been some studies to obtain these parameters. M. A. Hoang et al. propose that filter frequencies are obtained [20] from equation 9.

$$\begin{cases} F_L(i) = 0.25 - 2^{i-0.5}/N_c \\ F_H(i) = 0.25 + 2^{i-0.5}/N_c \end{cases} \quad (9)$$

Where F_L and F_H respectively are the low and high frequencies of filter cutting and N_c is the image width that is an integer power of two. The extracted texture features of Gabor filter can be the real part or size of the filter response and use of the non-linear Sigmoid function on the filter output. Gabor filters, due to the sensitivity of the direction and frequency, have become a popular tool in texture analysis. By using derived features from the partial images created by these filters, such as energy in different ways and different frequencies, we can diagnose and separate the different tissues from one another.

V. THE CLASSIFICATION AND DIAGNOSIS

For extracting suitable features, we use the Gabor filters bank in two directions, two frequencies, and two scales to identify the vessel. After pre-processing, first the image is divided into $[16 \times 16]$ windows and the Gabor filters are applied to each window. Thereupon, eight filtered images are obtained for each window.

The filters have been applied in the directions of $\pi/2$ and $\pi/4$, scales of 2 and 5, and two frequency of 0.5 and 2. Figures 4 and 5 show the applied Gabor filters. Then, the energy and entropy of these eight pictures of each sub-window are calculated and normalized. To calculate the energy and entropy of each sub-window, the 11 and 10 equations are used. Then, these teaching data are given to a perceptron with 20 neurons in the hidden layer to fully identify the prematureness and completeness of retinal images.

$$Energy = \sum_i \sum_j p(i, j)^2 \quad (10)$$

$$Entropy = -\sum_i \sum_j p(i, j) \log(p(i, j)) \quad (11)$$

In these equations, $p(i, j)$ is the pixel value at point i, j .

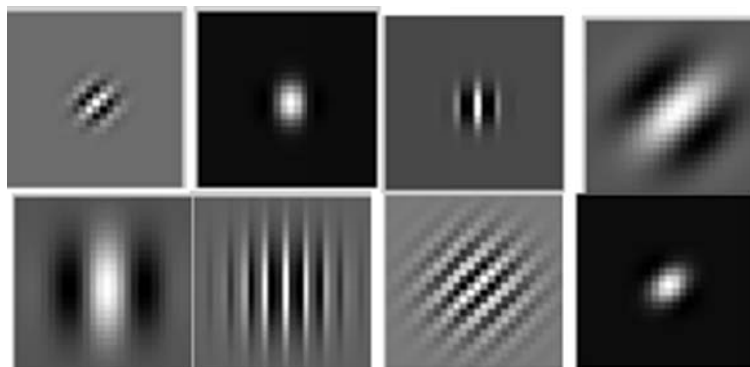


Fig. 4: Gabor filters in two directions, two scales and two frequencies

VI. RESULTS AND DISCUSSION

In this paper, for analyzing the results of the proposed methods, we used a public data set that is collected and labeled by a specialist. This data set contains 99 color images of the retina at different angles that are taken by an eye specialist center. These images are in 480×640 pixels size and are labeled with mature and immature. Table 1 shows the characteristics of the images in this collection. In order to evaluate the proposed method, this data collection has been used. Figure 5 displays an example of these eye images.

TABLE 1. The distribution of images in the photos data set

Number of pictures	Group / Label Image
79	immature
20	mature

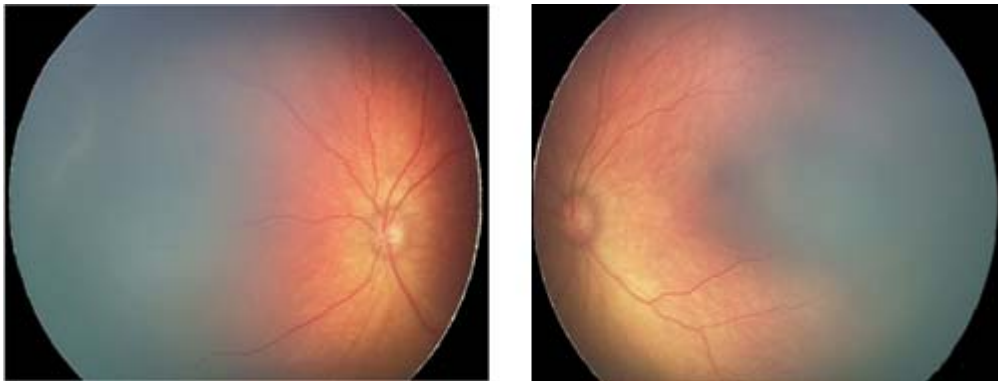


Fig. 5: An image example

Usually, three criteria are used to evaluate the medical diagnosis systems, such as accuracy (ACC), sensitivity (SNS) and specificity (SPC). These criteria are defined by equations 12, 13, and 14. Accuracy is the classified images ratio to the total images. The sensitivity shows the accuracy of the diagnosis of existence or absence of a disease. In classification systems, the accuracy criterion is used for evaluating the correctness of the overall system.

$$ACC = \frac{SNS + SPC}{2} \quad (12)$$

$$SNS = \frac{TP}{TP + FN} \quad (13)$$

$$SPC = \frac{TN}{TN + FP} \quad (14)$$

In these equations, TP^1 , TN^2 , FN^3 , and FP^4 respectively indicate the number of patients who have been identified patients, the number of healthy people who have been identified healthy, the number of patients who have been identified healthy and the number of healthy people who were detected as patients. The results which are presented to the neural network in different performances can be seen in Table 2.

TABLE 2. The obtained results in several different performance Perceptron.

Runs	MSE	Sensitivity%	Specificity%	Accuracy%
1	0.16	78	27	85
2	0.14	85.76	29.75	81.45
3	0.22	87.06	27.85	90.58
4	0.19	75.72	34.69	72.70
5	0.19	74.58	35.75	82.34
6	0.15	80.03	26.48	73.24
Average:	0.175	80.19	30.25	80.88

By evaluating the results, it is observed that the algorithm with the accuracy average of 80.88% and sensitivity of 80.19% is able to recognize the maturity and immaturity retinal images.

VII. CONCLUSION

In this paper, a method for early diagnosis of neonatal retinopathy was presented. Due to the lack of clarity of retinal blood vessels in neonates compared with adults, the blood vessel detection of retinal images in infants is more difficult than in adults. Therefore, in this paper, first in the preprocessing phase, the image contrast was improved by using the applied gamma transformation on the inverted green channel. Then, the $[16 \times 16]$ windows were removed from the image and Gabor filter was applied to each window. These Gabor filters were

applied in different directions and frequencies on each sub-window. Then, from each sub-window, the amount of energy and entropy was calculated and sent to perceptron neural network to determine the maturity or immaturity of the infants retina. The presented algorithm in this paper is able to detect the immaturity of retina with the accuracy of 80.88%. By using the presented method in this paper we can filter out the infants with high risk factors of ROP disease from other infants.

ACKNOWLEDGEMENT

This research is funded and supported by Universiti of Sains Malaysia (USM) and Institute of postgraduate studies (IPS). I would like to thank school of computer science to provide the facilities for this research.

REFERENCES

- [1] I. N. McRitchie, P. M. Hart, and R. J. Winder, (2006) "Image registration and subtraction for the visualization of change in diabetic retinopathy screening," *Computerized Medical Imaging and Graphics*, vol. 30, pp. 139-145.
- [2] W. L. Yun, U. Rajendra Acharya, Y. Venkatesh, C. Chee, L. C. Min, and E. Ng, (2008) "Identification of different stages of diabetic retinopathy using retinal optical images," *Information sciences*, vol. 178, pp. 106-121.
- [3] G. K. Matsopoulos, P. A. Asvestas, K. K. Delibasis, N. A. Mouravliansky, and T. G. Zeyen, (2008) "Detection of glaucomatous change based on vessel shape analysis," *Computerized Medical Imaging and Graphics*, vol. 32, pp. 183-192.
- [4] M. C. Castillo-Riquelme, J. Lord, M. J. Moseley, A. R. Fielder, and L. Haines, (2004) "Cost-effectiveness of digital photographic screening for retinopathy of prematurity in the United Kingdom," *International journal of technology assessment in health care*, vol. 20, pp. 201-213.
- [5] S. Chaudhuri, S. Chatterjee, N. Katz, M. Nelson, and M. Goldbaum, (1989) "Detection of blood vessels in retinal images using two-dimensional matched filters," *IEEE Trans on Med. Image.*, vol. 8, pp. 263-269.
- [6] J. J. Staal, M. D. Abr' amoff, M. Niemeijer, M. A. Viergever, and B. van Ginneken, (2004) "Ridge based vessel segmentation in color images of the retina," *IEEE Trans on Medical Imaging*, vol. 23(4): 501-509.
- [7] A. Fathi and A. R. Naghsh-Nilchi, "Automatic wavelet-based retinal blood vessels segmentation and vessel diameter estimation," (2013) *Biomedical Signal Processing and Control*, vol. 8, pp. 71-80.
- [8] A. Fathi, A. R. Naghsh-Nilchi, and F. A. Mohammadi, (2013) "Automatic vessel network features quantification using local vessel pattern operator," *Computers in biology and medicine*, vol. 43, pp. 587-593.
- [9] A. Fathi and A. R. Naghsh-Nilchi, (2013) "Integrating adaptive neuro-fuzzy inference system and local binary pattern operator for robust retinal blood vessels segmentation," *Neural Computing and Applications*, vol. 22, pp. 163-174.
- [10] J. V. B. Soares, J. J. G. Leandro, R. M. Cesar-Jr., H. F. Jelinek, and M. J. Cree. (2005) "Using the 2-Dmorlet wavelet with supervised classification for retinal vessel segmentation". In *IV Workshop de Teses e Dissertações em Computação Gráfica e Processamento de Imagens*, CD-ROM - 18th Brazilian Symposium on Computer Graphics and Image Processing, Natal, RN.
- [11] A. Fathi and A. R. Naghsh-Nilchi, (2014) "General rotation-invariant local binary patterns operator with application to blood vessel detection in retinal images," *Pattern Analysis and Applications*, vol. 17, pp. 69-81.
- [12] Fraz, M.M., Barman S. A., Remagnino P., Hoppe A., Basit A., Uyyanonvara B., Budnicka A. R., Owen C.G., (2012) "An approach to localize the retinal blood vessels using bit planes and centerline detection". *Computer Methods and Programs in Biomedicine*. Vol. 108:2. pp. 600-616.
- [13] Y. A. Tolias and S. M. Panas, (1998) "A fuzzy vessel tracking algorithm for retinal images based on fuzzy clustering," *Medical Imaging, IEEE Transactions on*, vol. 17, pp. 263-273
- [14] R. M. Rangayyan, F. J. Ayres, F. Oloumi, F. Oloumi, and P. Eshghzadeh-Zanjani, (2008) "Detection of blood vessels in the retina with multiscale Gabor filters," *Journal of Electronic Imaging*, vol. 17, pp. 023018-023018-7
- [15] Rafael C. Gonzalez, Richard E. Woods. *Digital Image Processing* (third edition). Prentice hall, (2008); pp. 48-120.
- [16] J.L. Starck, F. Murtagh, E. J. Candès, and D. L. Donoho, (2003) "Gray and Color Image Contrast Enhancement by the Curvelet Transform," *IEEE transactions on image processing*, vol. 12:6, pp. 706-717.
- [17] J. G. Daugman, (1985) "Uncertainty relation for resolution in space, spatial frequency, and orientation optimized by two-dimensional visual cortical filters," *Optical Society of America, Journal, A: Optics and Image Science*, vol. 2, pp. 1160-1169.
- [18] T. S. Lee, (1996) "Image representation using 2D Gabor wavelets," *Pattern Analysis and Machine Intelligence, IEEE Transactions on*, vol. 18, pp. 959-971.
- [19] A. K. Jain and F. Farrokhnia, (1991) "Unsupervised texture segmentation using Gabor filters," *Pattern recognition*, vol. 24, pp. 1167-1186.
- [20] M. A. Hoang, J. M. Geusebroek, and A. W. Smeulders, (2005) "Color texture measurement and segmentation," *Signal processing*, vol. 85, pp. 265-275.